Supporting Information

Barratt et al. 10.1073/pnas.0900689106

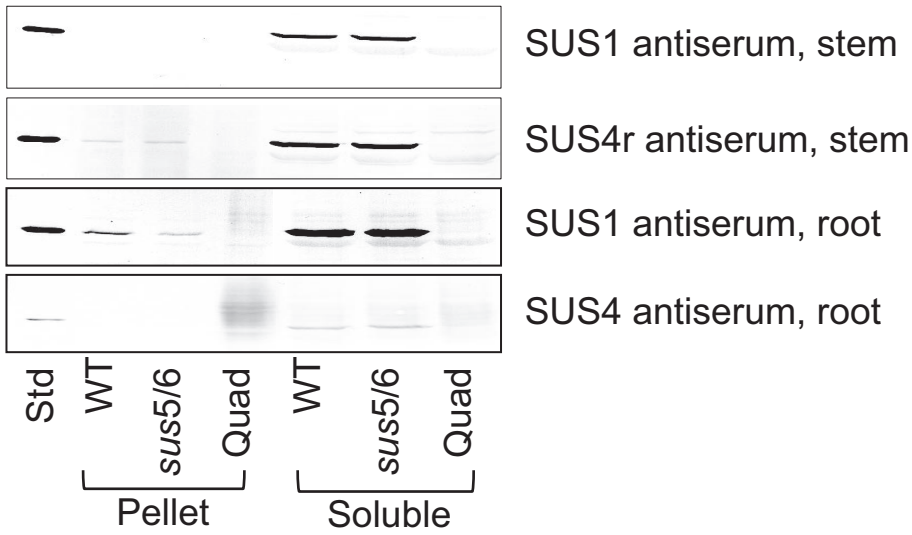

Fig. S1. Location of sucrose synthase (SUS)1 and SUS4 proteins in extracts of stems and roots. Immunoblots of extracts of stems and roots (as in Table 1) of WT, *sus5/sus6* and *sus1/sus2/sus3/sus4* (Quad) mutants, and purified SUS1 and SUS4 proteins (Std) were probed with antisera to SUS1 and SUS4. The purified protein was SUS1 for blots probed with SUS1 antiserum, and SUS4 for blots probed with SUS4 and SUS4r antiserum. The SUS1 antiserum recognizes SUS1 and no other SUS isoforms. The SUS4 antiserum recognizes both SUS4 and SUS3, but an antiserum specific for SUS3 does not recognize a SUS in either roots or stems; thus, the reaction of the SUS4 antiserum is likely to be specific for SUS4 in these extracts. The SUS4r antiserum recognizes both SUS4 and SUS1 (1). Pellet and soluble fractions were prepared by centrifugation of homogenates at 10,000 $\times$ *g* for 10 min. The pelleted material was washed twice with extraction medium by suspension and centrifugation before suspension in gel sample buffer. Extraction, gels, and blotting were as previously (1). For each panel, all lanes are from the same gel and blot, and contain the same amount of protein. Equal proportions of the soluble and solubilized, pelleted fractions were loaded onto the gel. Identical results were obtained with independent extracts.

1. Bieniawska Z, et al. (2007) Analysis of the sucrose synthase gene family in Arabidopsis. *Plant J* 49:810–828.

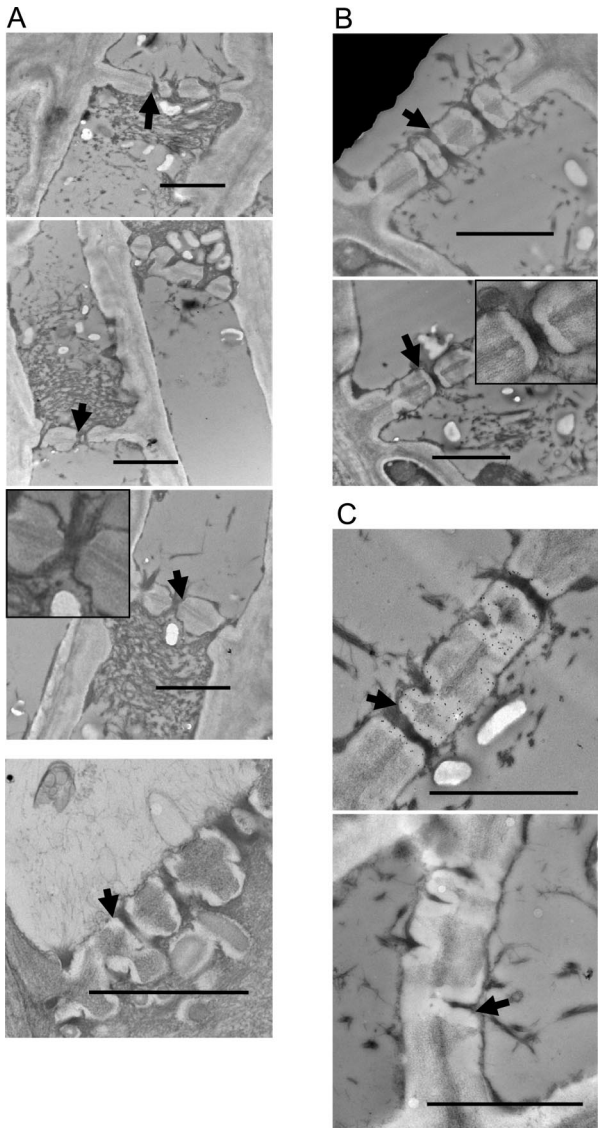

Fig. S2. Transmission electron micrographs of sieve elements in longitudinal sections of stems. The basal 4-cm section of the primary inflorescence stems of 6-week-old plants grown in compost was excised and immediately fixed. Samples were subjected to low-temperature embedding and stained with uranyl acetate (see below). Arrows indicate inner walls of the pores of sieve plates. Inserts are magnifications of arrowed regions. (Scale bars, 2 μm.) Pictures are typical of those obtained from several separate samples. (*A*) The *sus5/sus6* and quadruple mutant plants. Note the absence of an electron-transparent layer lining the sieve plate pores in the sus5/sus6 mutant (*Top* 3 images), and the presence of the layer in the quadruple mutant (*Bottom*). (*B*) WT plants. Note an electron-transparent layer lining every sieve plate pore. (*C*) Sections labeled with an anti-callose antiserum, followed by a gold-labeled second antiserum (*Upper*). Note the presence of gold particles (black dots) exclusively within the electron-transparent layer lining the sieve plate pores. No gold labeling is visible in a control sample where the anti-callose antiserum was omitted (*Lower*). Stems were cut at the base and immediately placed into fixative [2.5% (vol/vol) glutaraldehyde in 0.05 M sodium cacodylate, pH 7.3], sliced into 1-mm pieces, then placed in a vacuum infiltrator. Samples were incubated in fresh fixative and left overnight at room temperature. Subsequent steps used tissue-handling devices and low temperature to improve antigenicity (1). Infiltration steps were performed at −20 °C with LR White resin plus 0.5% (wt/vol) benzoin methyl ether, and polymerization was in Beem capsules, with indirect UV irradiation for 24 h at −20 °C then 16 h at room temperature. Sectioning was with a glass knife on a Leica UC6 ultramicrotome. Sections of ≈90 nm were picked up on pyroxylin- and carbon-coated 200 mesh copper grids, then stained with 2% (wt/vol) uranyl acetate for 1 h, washed in water, and air dried. Grids were viewed in a Jeol 1200 EX transmission electron microscope at 80 kV. For immunogold labeling, sections were picked up on pyroxylin- and carbon-coated gold grids. Grids were floated, section-side down, on 50 mM glycine/PBS (150 mM NaCl/10 mM phosphate, pH 7.4) for 15 min, then on Aurion blocking buffer (5% BSA/0.1% cold water fish gelatin/5–10% normal goat serum/15 mM NaN_3/PBS, pH 7.4) (Aurion) for 30 min, then briefly equilibrated in incubation buffer (0.1% (vol/vol) BSA-C (actetylated BSA; Aurion)/PBS, pH7.3) before incubation overnight at 4 °C with the primary antibody (to β1,3 glucan; Biosupplies) diluted to 1/10 in incubation buffer. Grids were washed for 5 min 5 times in incubation buffer, then placed on 1/50 goat anti-mouse secondary antibody conjugated to 10 nm gold (BioCell; Agar Scientific) diluted in incubation buffer, for 3–4 h. After 4- and 5-min washes in incubation buffer and 3- and 20-min washes in PBS with gentle agitation, the grids were washed in water twice for 30 min, then contrast stained with uranyl acetate.

1. Wells B (1985) Low temperature box and tissue handling device for embedding biological tissue for immunostaining in electron microscopy. *Microsc Acta* 16:49–53.

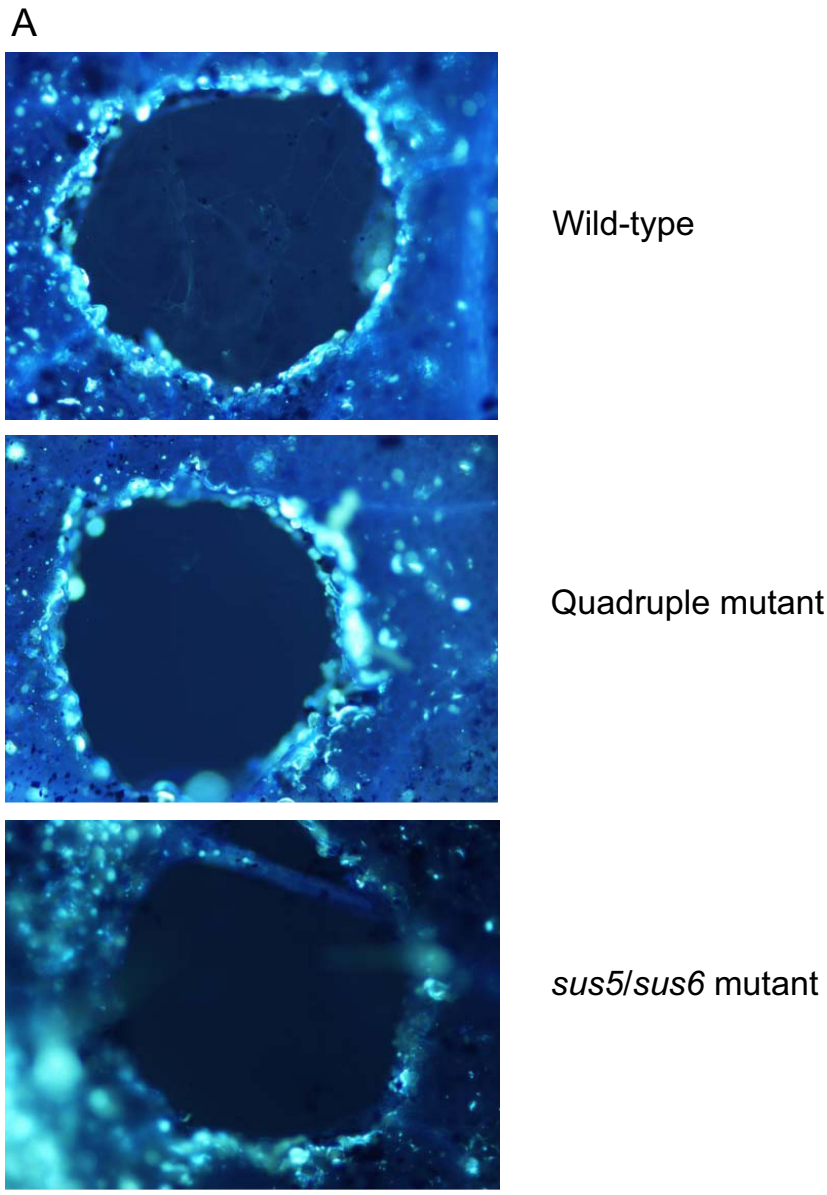

Fig. S3. Presence of callose after wounding and associated with plasmodesmata of leaves. Experiments were done on mature, nonflowering rosettes. Callose was stained with aniline blue, and appears as blue fluorescence. (*A*) Callose synthesis after wounding. Note the presence of callose surrounding puncture sites in leaves of WT (*Top*), quadruple mutant (*Middle*), and *sus5*/*sus6* mutant (*Bottom*) plants. Fully expanded leaves from 6-week-old plants were punctured with a plastic tip, then harvested the next day and subjected to several washes in methanol to remove all chlorophyll. After rinsing in water, leaves were stained overnight in 0.05% (wt/vol) aniline blue in 50 mM K phosphate pH 8.0 and viewed with a UV epifluorescence microscope. (*B*) WT panels. Callose associated with plasmodesmata between mesophyll cells (*Upper*) and between epidermal cells (*Lower*). (*Left*) Sample imaged for callose fluorescence. (*Center*) Sample viewed with transmitted light. (*Right*) Overlay of *Left* and *Center*. Quadruple mutant panels. Callose associated with plasmodesmata between epidermal cells. (*Left*) Sample imaged for callose fluorescence. (*Center*) Sample viewed with transmitted light. (*Right*) Overlay of *Left* and *Center*. The *sus5*/*sus6* mutant upper panels. Callose associated with plasmodesmata between epidermal cells. (*Left*) Sample imaged for callose fluorescence. (*Center*) Sample viewed with transmitted light. (*Right*) Overlay of *Left* and *Center*. The *sus5*/*sus6* mutant lower panels. Callose associated with plasmodesmata between mesophyll cells. (*Upper Left*) Sample imaged for callose fluorescence. (*Upper Right*) Sample viewed with transmitted light. (*Lower Left*) Sample imaged for chlorophyll fluorescence. (*Lower Right*) Overlay of the preceding three panels. Fully expanded detached leaves from 7-week-old plants were pressure infiltrated with a 2:3 vol/vol mixture of 0.1% (wt/vol) aniline blue and 1 M glycerol at pH 9.5, and viewed after 10 min by using excitation and emission wavelengths of 405 and 460–500 nm, respectively. Chlorophyll autofluorescence used excitation and emission wavelengths of 488 and 670–690 nm, respectively.

B

Wild-type

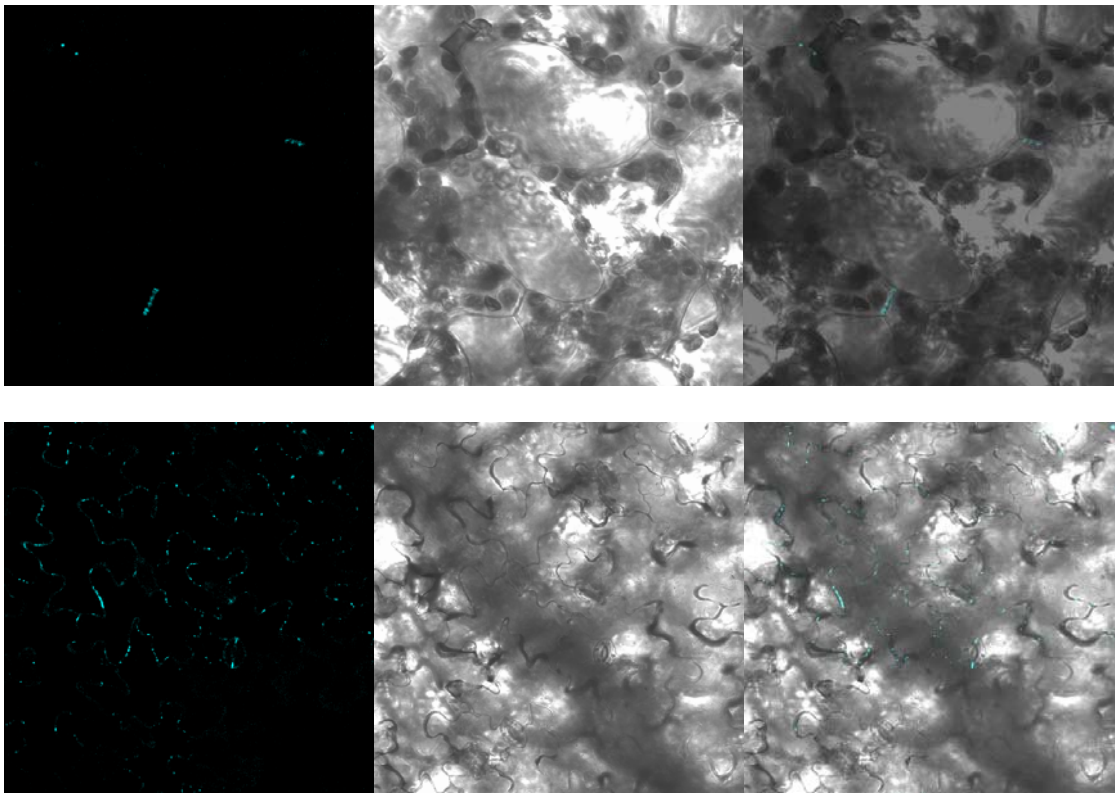

Quadruple mutant

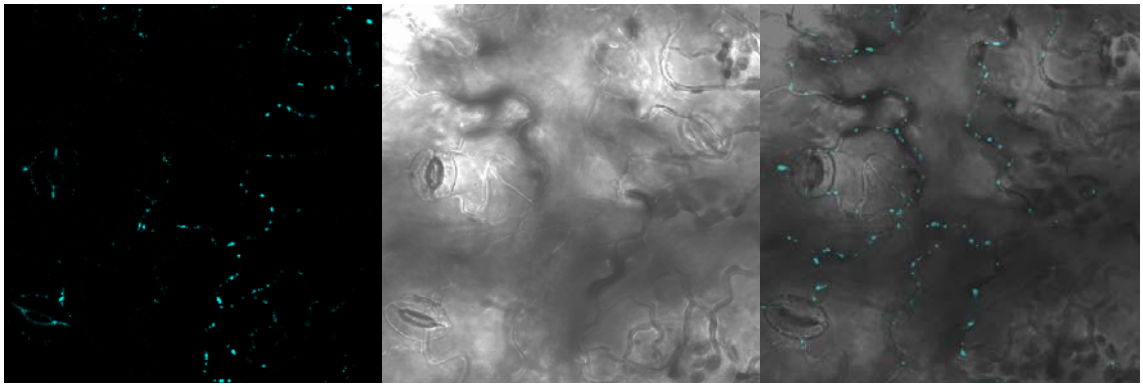

Fig. S3. (continued).

sus5/*sus6* mutant

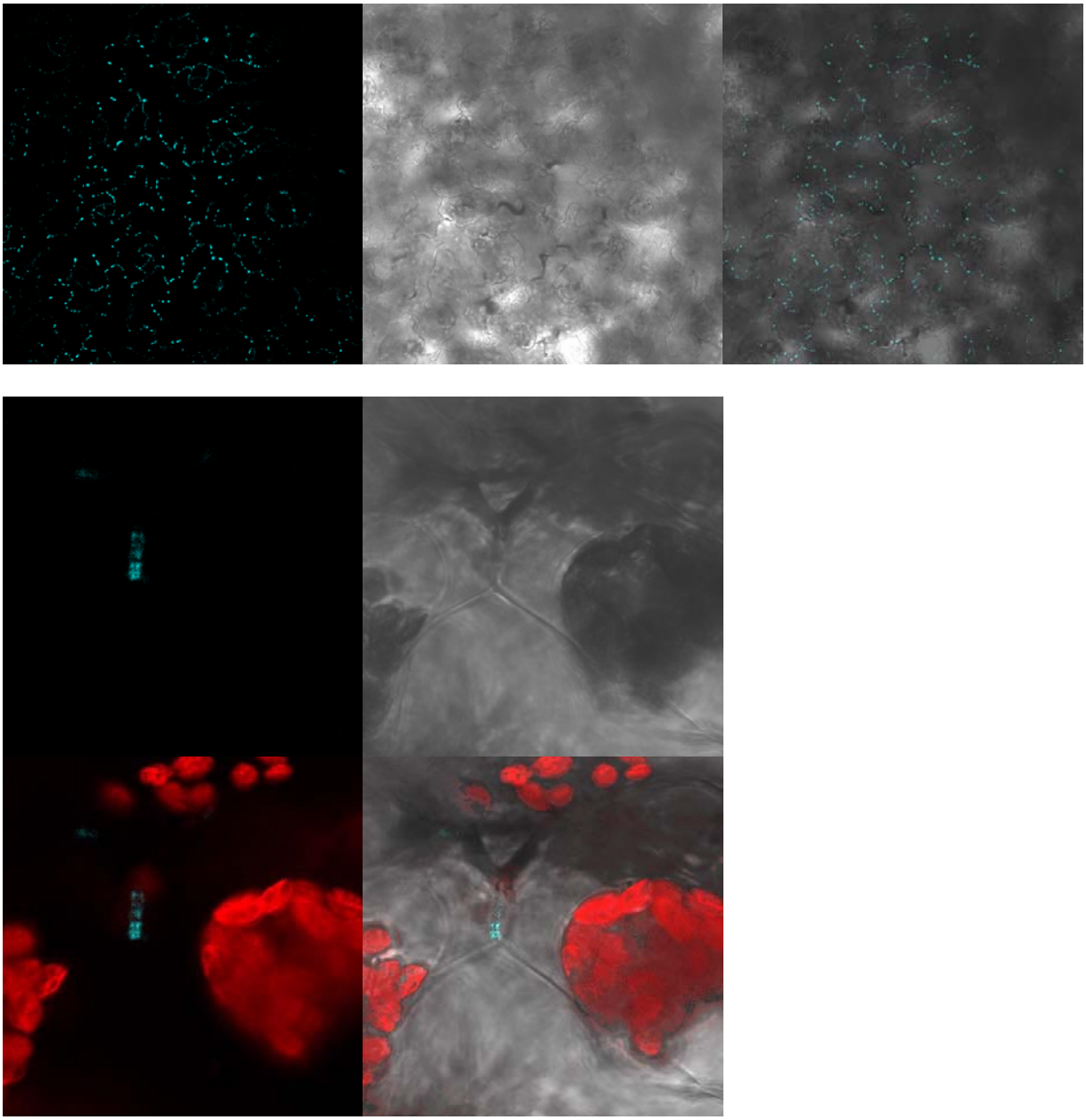

Fig. S3. (continued).

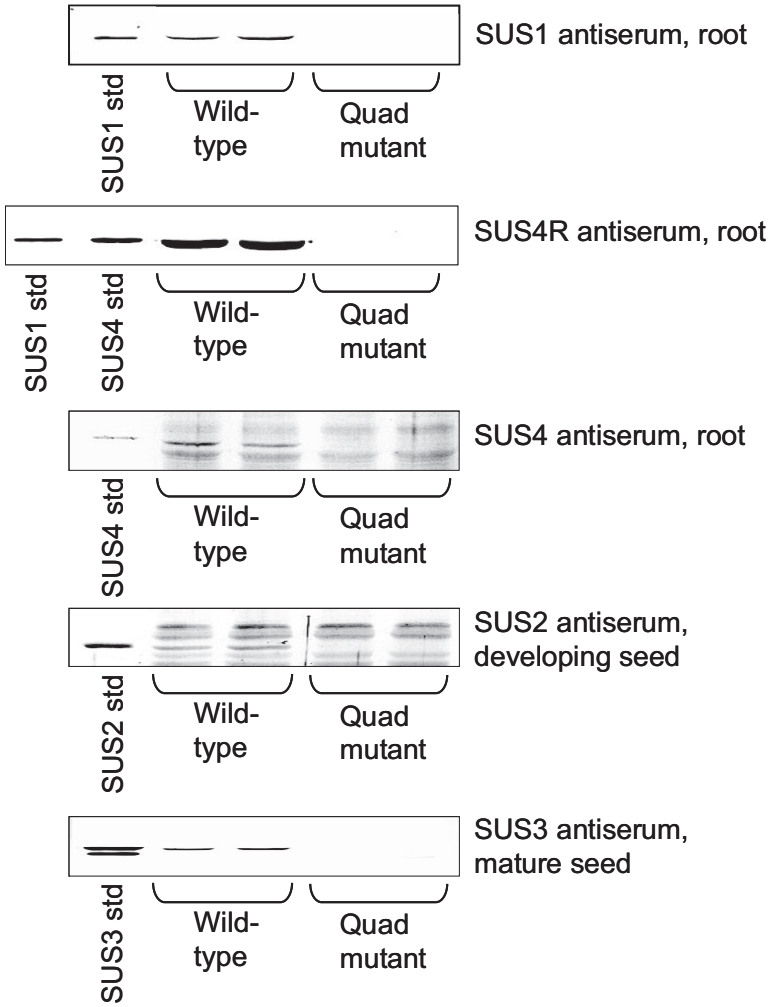

Fig. S4. Absence of SUS proteins 1 to 4 from the quadruple mutant. Immunoblots of the soluble fraction (after a 10,000 × *g* centrifugation) of extracts of roots (from 4-week-old plants grown as in Table 1), developing seeds (11–15 days after flowering), and mature seeds of WT and *sus1/sus2/sus3/sus4* (Quad) mutants, and purified SUS proteins as indicated (std), were probed with antisera to SUS isoforms. SUS1, SUS4, and SUS4r antisera are described in Fig. S1. SUS2 and SUS3 antisera were specific for the respective isoforms (1). Each lane contains the same amount of protein. Each of the 5 strips is from a single blot. Identical results were obtained with independent extracts.

1. Bieniawska Z, et al. (2007) Analysis of the sucrose synthase gene family in Arabidopsis. *Plant J* 49:810–828.

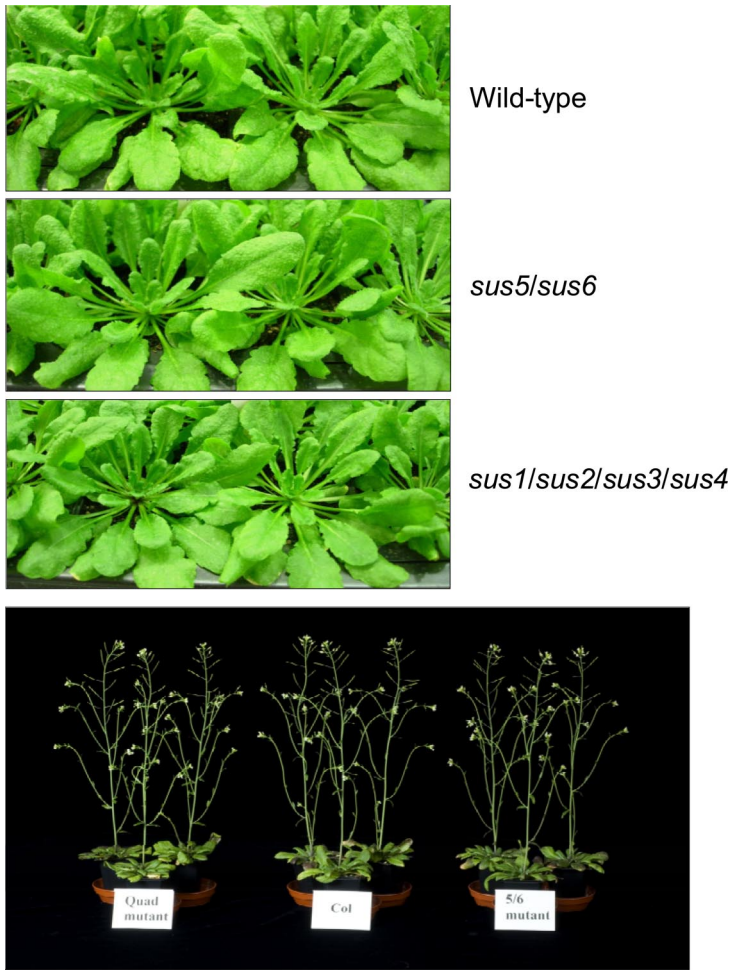

Fig. S5. WT, *sus5/sus6*, and quadruple mutant plants. (*Upper*) Plants were grown in 9-h light, 15-h dark at 95 μmol quanta m^{-2} s^{-1}. (*Lower*) Plants were grown in 12-h light, 12-h dark at 180 μmol quanta m^{-2} s^{-1}.

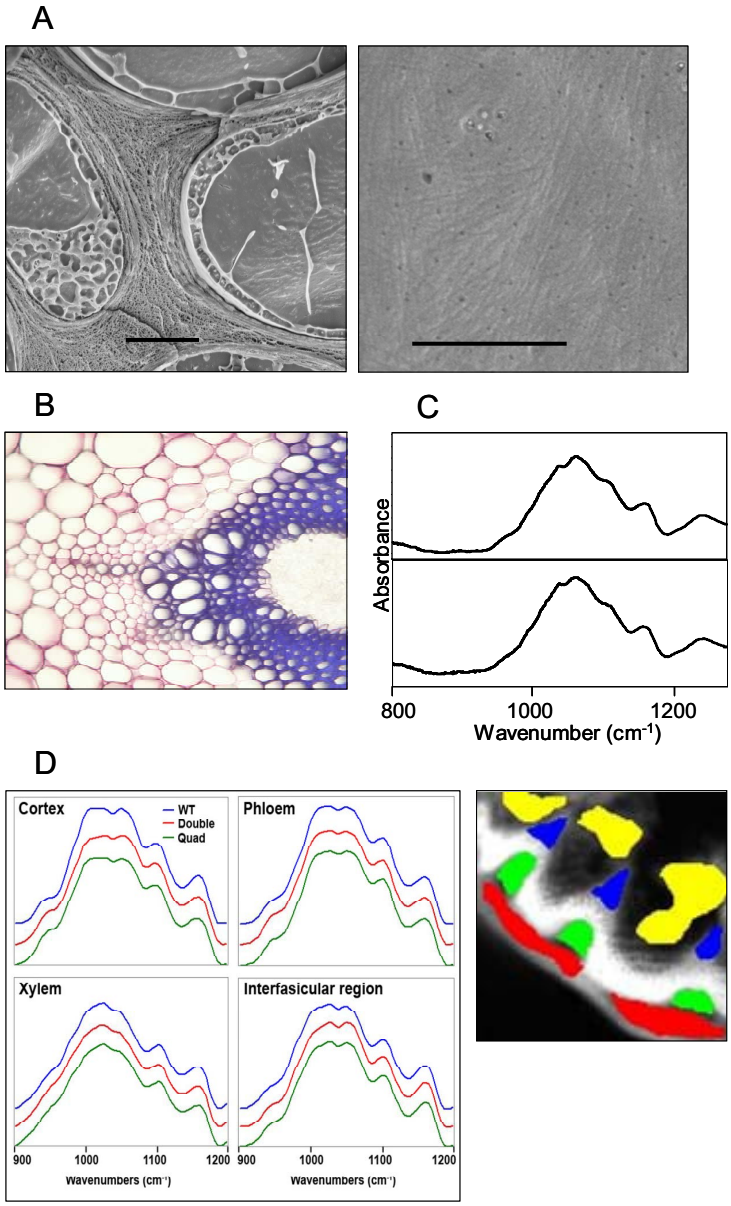

Fig. S6. Leaf and stem anatomy and FTIR analysis of the *sus5*/*sus6* mutant. (*A*) Scanning electron micrographs of freeze-fractured rosette leaves, showing cell walls in cross section (Scale bar, 2 μm.) (*Left*), and face-on (Scale bar, 1 μm.) (*Right*). (*B*) Light micrograph of cross-sections of the basal 4 cm of a flowering stem, as in Fig. 2. Sections of 30-μm thickness were prepared and imaged as for Fig. 2. (*C*) Spectra from FTIR analyses of cell walls. Spectra were derived from the insoluble fraction of homogenized roots of seedlings. Samples were dried between 2 barium fluoride disks under a 500 g load for 3 days. Disks were mounted on the stage of a Digilab UMA600 microscope interfaced to a Digilab FTS6000 FTIR spectrometer (Varian). The spectra are averaged from analyses on 20 samples from a preparation made from 40 primary roots. (*Upper*) WT roots (as in Fig. 2). (*Lower*) The *sus5*/*sus6* roots. Very similar results were obtained in an independent set of experiments on a different batch of seedlings. In addition to comparisons of spectra, we calculated the ratio of absorbances at 1,056 and 1,100 cm^{-1} (which reflects the pectin to cellulose ratio of cell-wall material) (1). This was the same in WT and mutant plants. For example, in 1 experiment, the ratio was 0.72 $\pm$ 0.02 and 0.68 $\pm$ 0.02 for root cell walls from WT and quadruple mutant seedlings, respectively (mean $\pm$ SD, 20 scans of preparations from 40 5-day-old seedlings; a further experiment gave similar results). (*D*) Scanning FTIR array microscopy on stem sections. FTIR imaging was performed with a 128 by 128 pixel ''Stingray'' detector, with each pixel measuring 5 $\times$ 5 μm. Data from 32 scans at 8 cm^{-1} were averaged and referenced against spectra from an empty area of the disc. Data from 7 sections per genotype were analyzed with ENVI 4.3 (ITT Visual Information Solutions). The average spectra for regions representing different tissue types were computed, then spectra from the individual sections were baseline-corrected and averaged. Choice of wavenumbers for analysis was dictated by available information (2). (*Left*) Averaged spectra for WT, *sus5*/*sus6* mutant (Double), and *sus1*/*sus2*/*sus3*/*sus4* mutant (Quad) stems, for the regions indicated. Values on the *y* axis are relative: spectra have been separated to allow individual inspection. (*Right*) Areas scanned on one section: red is cortex; green, phloem; blue, xylem; and yellow, interfascicular region.

1. Cael JJ, Gardner KH, Koenig JL, Blackwell J (1975) Infrared and Raman spectroscopy of carbohydrates. Normal coordinate analysis of cellulose. *J Chem Phys* 62:1145–1153.
2. Kacurakova M, Capek P, Sasinková V, Wellner N, Ebringerová A (2000) FT-IR study of plant cell wall model compounds: pectic polysaccharides and hemicelluloses. Carbohydr Polym 43: 195–203.

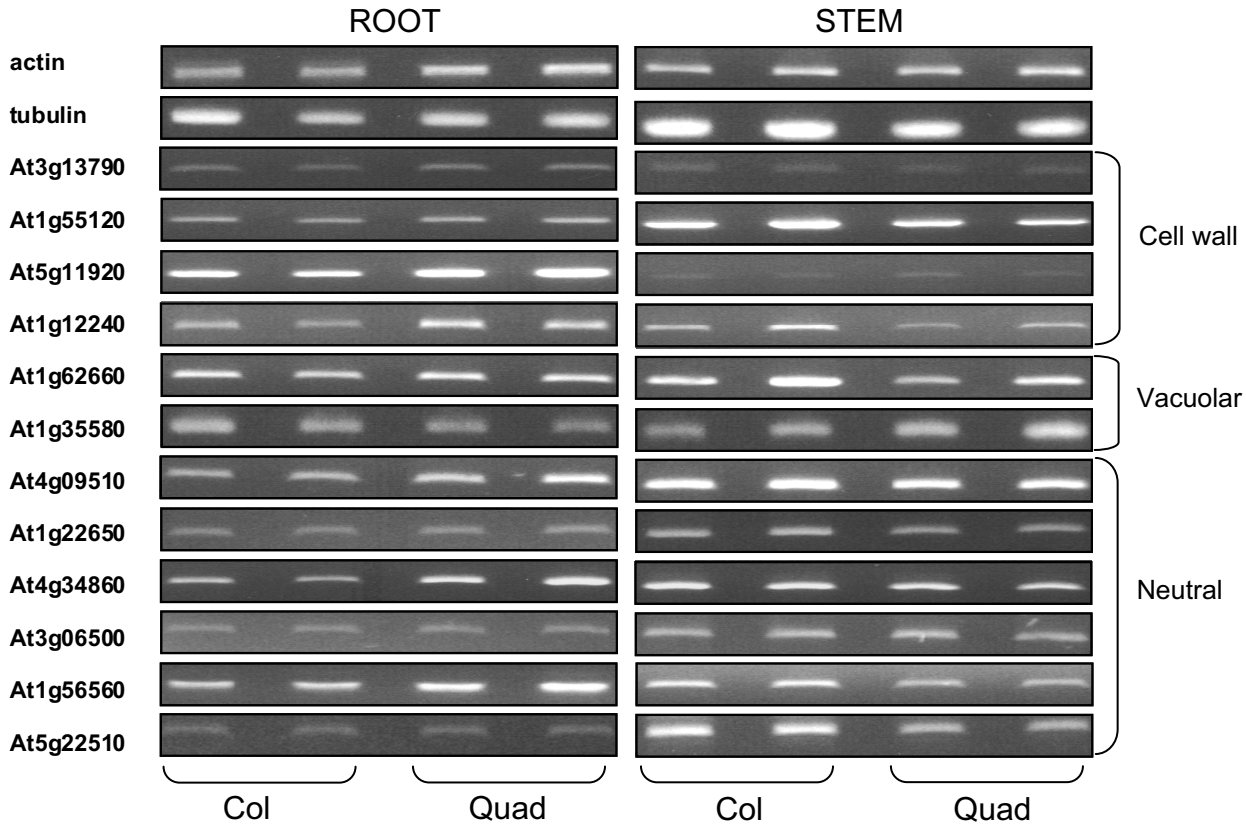

Figure S7. Semiquantitative RT-PCR analysis of invertase transcripts. Semiquantitative RT-PCR analysis was performed for the 12 most highly expressed invertase (INV) isoforms in roots and stems (based on data from Genevestigator, https://www.genevestigator.ethz.ch/gv/index.jsp) (1). The figure shows that none of these transcripts was elevated in stems or roots of the mutant plants. We previously found no major differences in leaf or root activity of neutral and acid INV between WT plants and the double mutants *sus1/sus4*, *sus2/sus3* and *sus5/sus6* (2). Total RNA was isolated (2) from 5-week-old roots (grown as in Table 1) and from the basal 4-cm section of the main inflorescence stem of 6-week-old plants (grown as Table 1). Plants were either WT (Col) or the quadruple mutant *sus1/sus2/sus3/sus4* (Quad). Each boxed section of the figure is a single photograph of contiguous tracks from a single gel. Each experiment was repeated at least twice with 2 or more independent biological replicates: the 2 bands for each genotype are from RNA preparations from 2 different biological samples. For tubulin and actin, each band was from the same RNA preparation as the invertase bands directly below it. First-strand cDNA was synthesized from 5 μg of total RNA (2). Primers for the genes encoding actin and tubulin were used as standards for mRNA expression; all RT-PCR for the different genes were from the same cDNA samples. The following primers were used: actin: 5′-CTTCCTCAATCTCATCTTCT-3′ and 5′-TTAACATTGCAAAGAGTTTCAAGGT-3′; tubulin: 5′-CCTGATAACTTCGTCTTTGG-3′ and 5′-GTGAACTCCATCTCGTCCAT-3′; cell-wall invertases: At3g13790, 5′-GACTTTGGTTATTGCTCACGTTACTTATTG-3′ and 5 ′-CAACGTACTTATTGCTGTTTTGACGGGCTT-3′; At1g55120, 5′-AAGCTTCTTCTCATCAAGATCTCAACCAAC-3′ and 5 ′-TCAAAACTGATGATTAGGTGAGCGTGACTC-3′; At5g11920, 5′-ATGGAACAGAATCTTCTTCAAACCGCTGTG-3′ and 5′-AAGTTGGGTTTGAATTGATTTGGGCATTTC-3′; vacuolar invertases: At1g12240, 5′-TTGCCAATCTCCGCCAGAGAAGAAGAACCA-3′ and 5′-GTACGGGAGAGAGCACGGACAGCTTCGTCA-3′; At1g62660: 5′-ACCCGTCACGTCCCTACAAGATCCATTATC-3′ and 5′-GTGCTGGAAGGAACACCGAGATCGTCTGAA-3′; Alkaline/neutral invertases: At1g35580, 5′-ATGGAAGGTGTTGGACTAAGAGCTGTAGGA-3′ and 5′-AGTTGTGGCCAAGACGCAGATCGCTTGATG-3′; At4g09510, 5′-CATAAAGAACCATTGGTGCTAAGAGTTGAA-3′ and 5′-CAAGTCCATGAAGCAGATCTCTTGATAACA-3′; At1g22650, 5′-GTAAACTCTTCAAGCTCTATATCCGACCTA-3′ and 5′-AGTCCAAGAATAAGATCTCTTAATGACAGG-3′; At4g34860, 5′-AGTTTTAATCTGAGTGTAGATGTGAATCAG-3′ and 5′-CAAGTCCAGGAGTTGGATCTTCTCATAACG-3′; At3g06500, 5′-ATGAACAGTAGAAGCTGTATCTGTGTCTCT-3′ and 5′-GATCTTGGAGGTGTGAAACGCGAACACTTG-3′; At1g56560, 5′-GAGCGCAATCTATCTCCTCCGCAAAATTTC-3′ and 5′-TCGAACAAGAATCTGAGTCTTGGCAGCGAC-3′; At5g22510, 5′-TGGCAGCTTCAGAAACAGTTCTACGTGTTC-3′ and 5′-TTGAGCTTTTTTGGGTCCTCTTGTCCTCCT-3′. Different amplification cycles were performed for the different genes and tissues to avoid saturation of the reaction. The following conditions were established: tubulin, 24 cycles; actin, root 24 cycles, stem 22 cycles; At3g13790, root 24 cycles, stem 28 cycles; At1g55120, 28 cycles; At5g11920, 28 cycles; At1g12240, root 25 cycles, stem 22 cycles; At1g62660, root 24 cycles, stem 28 cycles; At1g35580, 24 cycles; At4g09510, 28 cycles; At1g22650, 28 cycles; At4g34860, 28 cycles; At3g06500, 24 cycles; At1g56560, root 28 cycles, stem 24 cycles; and At5g22510, 24 cycles. Ten μL of each product were separated by electrophoresis on a 1% (w/v) agarose gel and stained with ethidium bromide.

1. Sergeeva LI, et al. (2006) Vacuolar invertase regulates elongation of *Arabidopsis thaliana* roots as revealed by QTL and mutant analysis. *Proc Natl Acad Sci USA* 103:2994–2999.
2. Bieniawska Z, et al., (2007) Analysis of the sucrose synthase gene family in Arabidopsis. *Plant J* 49:810–828.
3. Turner SR, Somerville CR (1997) Collapsed xylem phenotype of Arabidopsis identifies mutants deficient in cellulose deposition in the secondary cell wall. *Plant Cell* 9:689–70142.

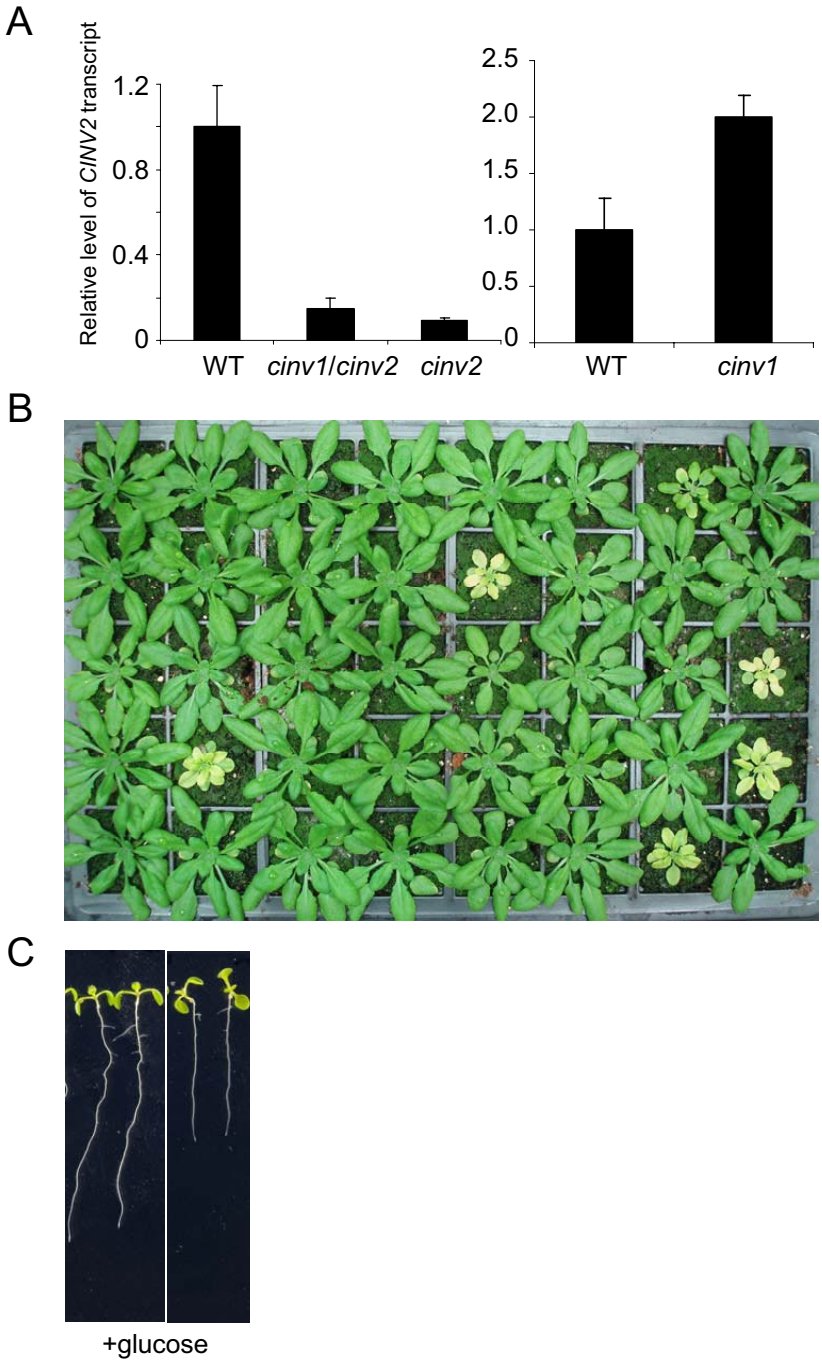

Figure S8. Analysis of the *cinv1*/*cinv2* double mutant. (*A*) Relative transcript levels for *CINV2*; cDNA was synthesized from RNA from 9-day-old seedlings grown on solid medium with 1% (w/v) sucrose, and subjected to quantitative RT-PCR analysis (DNA Engine Optican 2 Real-Time PCR Detection System; Biorad) in a reaction mix containing 5 μL SYBR Green JumpStartTM (Sigma), 1 μL cDNA and 2 μL of each gene-specific primer. Thermal cycling was: 95 °C for 2 min, 40 cycles of 95 °C for 10 s, 60 °C for 1 min. Primers for *CINV2* were: f 5′ GGGTTACTTGGTTGCGAAAA; r 5′ CAGCAAGTCCATGAAGCAGA. Values were normalized against a *UBIQUITIN10* control, and relative expression was calculated by setting the WT value to 1. (*Left*) Comparison of levels of *CINV2* transcript in WT, *cinv1*/*cinv2*,and *cinv2* seedlings. (*Right*) Comparison of levels of *CINV2* transcript in WT and *cinv1* seedlings. Values are means of measurements on 3 preparations of cDNA, each from a separate batch of roots. Bars represent SD. The WT value is statistically significantly different from the double and *cinv2* values ($P < 0.002$) and from the *cinv1* value ($P = 0.008$; Student's *t* test). (*B*) Appearance of a segregating, F2 population from a cross between *cinv1* and *cinv2*. All of the small plants are *cinv1*/*cinv2* mutants. (*C*) Appearance of seedlings grown on vertical plates containing 1% (w/v) glucose. (*Left*) WT seedlings. (*Right*) The *cinv1*/*cinv2* seedlings. Note the much greater root extension in *cinv1*/*cinv2* seedlings in the presence of glucose than in its absence (shown in Fig. 3). Seedlings were all from the same plate, were photographed at the same time, and are at the same magnification.

Table S1. Starch, sucrose, and sucrose catabolites in leaves, roots, stems, and siliques

	Content, μmol g^{-1} fresh weight									
	Leaves				Roots		Stems		Siliques	
	End of day		End of night							
Metabolite	WT	Quad	WT	Quad	WT	Quad	WT	Quad	WT	Quad
Starch	*	*	*	*	*	*	1.01 ± 0.16	0.91 ± 0.09	71 ± 7	107 ± 11
Sucrose	*	*	*	*	*	*	0.41 ± 0.03	0.46 ± 0.01	22 ± 0.4	20 ± 0.2
Glucose	*	*	*	*	*	*	2.49 ± 0.4	2.30 ± 0.49	6.9 ± 0.4	4.6 ± 0.2
Fructose	*	*	*	*	*	*	0.45 ± 0.05	0.41 ± 0.06	3.56 ± 0.27	3.18 ± 0.14
Content, nmol g^{-1} fresh weight										
Glucose 6-P	206 ± 6	229 ± 5	132 ± 9	142 ± 7	113 ± 6	92 ± 25	242 ± 15	238 ± 12	462 ± 32	540 ± 74
Fructose 6-P	54 ± 2	57 ± 3	40 ± 7	35 ± 2	28 ± 2	21 ± 6	57 ± 5	58 ± 4	79 ± 7	70 ± 8
Glucose 1-P	19 ± 2	27 ± 7	17 ± 3	15 ± 2	9.1 ± 1.6	7.4 ± 1.6	7.3 ± 1.2	11.5 ± 1.8	73 ± 18	70 ± 6
UDPglucose	63 ± 3	76 ± 1	56 ± 5	63 ± 3	39 ± 2	32 ± 7	62 ± 3	62 ± 3	59 ± 4	77 ± 18

Metabolite contents of organs of WT and quadruple mutant (Quad) plants. Starch, sucrose and sucrose catabolites in various organs. Plants were grown under 12-h light, 12-h dark at 20 °C. For leaves, whole rosettes from compost-grown, 4-week-old plants were harvested into liquid nitrogen at the start and at the end of the light period (end of night and end of day, respectively). For roots, roots systems were cut at the end of the light period from 4-week-old plants grown in sand:Terragreen, rinsed, and blotted very briefly, then frozen in liquid nitrogen. For stems, 4-cm sections were cut from the base of the primary inflorescence of 6-week-old plants grown in compost. Each sample consisted of stems from 3 plants. For siliques, material was harvested from compost-grown plants, ≈5 h into the photoperiod. Each sample consisted of 9 siliques (9 to 11 days after flowering), taken from a single plant. Frozen material was extracted in dilute perchloric acid. After neutralization, extracts were assayed enzymatically for metabolites. Values are means ± SE of measurements on 5 or 6 samples. Asterisks indicate data provided in Table 1.

Table S2. Other metabolites in leaves

Metabolite	Content, nmol g^{-1} fresh weight	
	WT	Quad
ADPglucose	0.07 ± 0.04	0.08 ± 0.03
Sucrose 6-phosphate	0.122 ± 0.045	0.145 ± 0.047
Trehalose 6-phosphate	0.137 ± 0.023	0.149 ± 0.033
Glycerate	1042 ± 153	1079 ± 210
3-PGA + 2-PGA	185 ± 37	185 ± 33
Glyceraldehyde 3-phosphate	3.51 ± 0.36	3.60 ± 0.66
Phosphoenolpyruvate	12.9 ± 3.0	13.7 ± 4.8
Pyruvate	47.6 ± 14.1	46.7 ± 10.7
2-Oxoglutarate	135 ± 29	139 ± 31
Citrate	5459 ± 1161	5852 ± 1014
Malate	1747 ± 371	1735 ± 348
Succinate	54 ± 24	47 ± 18
Fumarate	2398 ± 485	2352 ± 530
Aconitate	73 ± 13	73 ± 13
Shikimate	13.7 ± 2.5	14.3 ± 3.8

Metabolite contents of WT and Quad leaves. Plants were grown under 12-h light, 12-h dark for 4 weeks at 20 °C. Whole rosettes were harvested into liquid nitrogen 4.5 h into the photoperiod. Frozen material was extracted in chloroform-methanol (3:7, v/v), and metabolites were analysed by LC-MS/MS. Values are means ± SD of measurements on 12 rosettes. PGA, phosphoglycerate.